

## Removal of Malachite Green from Dye Wastewater Using Mesoporous Carbon Adsorbent

M. Anbia\* and A. Ghaffari

Research Laboratory of Nanoporous Materials, Faculty of Chemistry, University of Science and Technology, Narmak, Tehran 16846, Iran

(Received 8 January 2010, Accepted 21 May 2010)

Mesoporous carbon was synthesized for the removal of a cationic dye malachite green (MG) from aqueous solution. The studies were carried out under various experimental conditions such as contact time, dye concentration, adsorption dose and pH to assess the potentiality of mesoporous carbon for the removal of malachite green dye from wastewater. The sorption equilibrium was reached within 30 min. In order to determine the adsorption capacity, the sorption data were analyzed using linear form of Langmuir and Freundlich equation. Langmuir equation showed higher conformity than Freundlich equation. More than 99% removal of MG was reached at the optimum pH value of 8.5. From kinetic experiments, it was concluded that the sorption process followed the pseudo-first-order kinetic model. This study showed that mesoporous carbon can be recommended as an excellent adsorbent at high pH values.

**Keywords:** Adsorption isotherm, Kinetic study, Malachite green dye, Mesoporous carbon adsorbent

### INTRODUCTION

The wastewater coming out from the textile industries causes major hazards to the environment due to the presence of a large number of contaminants like acids, bases, toxic organic and inorganic compounds, dissolved solids and colors. Dyes removal from wastewater is the main problem encountered in textile industry. Most of the dyes, including malachite green, are toxic and must be removed before discharge into receiving streams. Malachite green (MG) is an N-methylated diaminotriphenylmethane dye (Fig. 1).

MG is one such dye used extensively in textile industry for dyeing silk, leather, cotton, wool and jute. It is also extensively used as a bactericide, fungicide and parasiticide in aquaculture industries worldwide. MG is highly toxic to

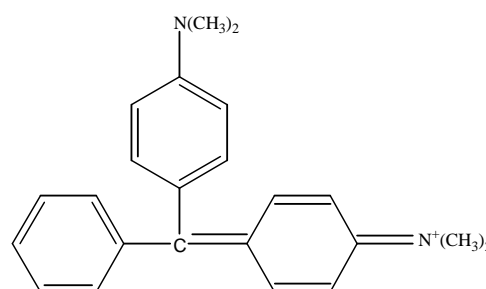


Fig. 1. Chemical structure of malachite green.

mammalian cells and causes kidney tumors in mice and reproductive problems in rabbit and fish [1]. Various attempts have been made for its removal from the wastewater. These include photo-degradation [2,3], photo-catalytic degradation [4-6] and adsorption.

\*Corresponding author. E-mail: anbia@iust.ac.ir

Among the various treatment methods, adsorption is found to be the versatile process and gives best results in the treatment of the colored dyestuff effluents. Most of the investigations are based on commercial activated carbon and activated carbon derived from various sources, but activated carbons prepared by activation of biomass are fundamentally microporous [7], which limits their adsorption capacity of dyes since dyes are bulky molecules with sizes of over 1 nm [8-10]. Therefore, carbons with mesoporous structures are advantageous.

In 1992, the discovery of the ordered mesoporous material MCM-41 opened up a new research field in mesoporous materials that were highly desirable for application in processes that involve large molecules [11-14]. Nowadays, mesoporous carbon materials with ordered pore structure, high pore volume, high specific surface area, and tunable pore diameters can be prepared using the hard template method [15]. Due to its open pore structure and mesoporous properties, mesoporous carbon provides marked advantages over typical activated carbon in the adsorption and diffusion process [16]. Recently, the adsorption of bulky pollutants using mesoporous carbon was reported [17-19]. Whilst the above materials have remarkable textural characteristics, with the best of our knowledge, no study of malachite green adsorption on ordered mesoporous carbon materials has been reported until now.

In this work we report the adsorption of MG on ordered mesoporous carbon (OMC), and the results are compared with mesoporous silica (MCM-48) and other adsorbents. Moreover, the effect of the pH, contact time and initial concentration on the amount of MG adsorption on mesoporous carbon adsorbent is also reported. It was found that OMC shows fairly good adsorption for MG. Freundlich and Langmuir adsorption isotherms were used to model the equilibrium adsorption data for MG.

## EXPERIMENTAL

### Materials

The reactants used in this study were malachite green; tetraethyl orthosilicate (TEOS) as a silica source, cetyltrimethylammonium bromide (CTAB) as a surfactant, sodium hydroxide (NaOH), sodium fluoride (NaF), and

deionized water for synthesis of mesoporous silica (MCM-48); sucrose as the carbon source and sulfuric acid as a catalyst for synthesis of mesoporous carbon. All chemicals were analytical grade from Merck.

### Synthesis of Mesoporous Silica (MCM-48)

MCM-48 was prepared according to the synthesis procedure described by Yaofeng Shao [20]. In a representative synthesis, the MCM-48 molecular sieve was prepared as follows: 10 ml of tetraethyl orthosilicate (TEOS) was mixed with 50 ml of deionized water, and the mixture was vigorously stirred for 40 min at 308 K. Afterwards, 0.9 g of NaOH and 0.19 g of NaF were added into the mixture, respectively. After another 60 min of vigorously stirring, 10.61 g of cetyltrimethylammonium bromide (CTAB) was added to the mixture, and stirring continued for 60 min. The mixture was heated for 24 h at 393 K in an autoclave under static conditions, and the resulting product was filtered, washed with distilled water and dried at 373 K. The as-synthesized samples were then calcined in air for 4 h at 823 K, increasing the temperature to 823 K at  $1\text{ }^{\circ}\text{C min}^{-1}$  of the heating rate.

### Synthesis of Ordered Mesoporous Carbon (OMC)

OMC was prepared according to the synthesis procedure described by Riong Ryoo [21]. In a representative synthesis, the OMC molecular sieve was prepared as follows: 1.25 g sucrose and 0.14 g  $\text{H}_2\text{SO}_4$  were dissolved in 5.0 g  $\text{H}_2\text{O}$ , and the solution was added to 1 g MCM-48. The resultant mixture was dried in an oven at 373 K, and subsequently, the oven temperature was increased to 433 K. The mixture was heated at this temperature for 6 h and then the resulting MCM-48 silica containing the partially carbonizing organic masses was added to an aqueous solution consisting of 0.75 g sucrose, 0.08 g  $\text{H}_2\text{SO}_4$  and 5.0 g  $\text{H}_2\text{O}$ . The resultant mixture was dried again at 373 K, and subsequently the oven temperature was increased to 433 K. The color of the sample turned to very dark brown or nearly black. This powder sample was heated to 1173 K under vacuum using a fused quartz reactor equipped with a fritted disk. The carbon-silica composite thus obtained was washed with 1 M NaOH solution of 50% ethanol- 50%  $\text{H}_2\text{O}$  twice at 363 K, in order to dissolve the silica template completely. After the silica removal, the obtained carbon samples were filtered, washed with ethanol and dried at 393 K.

## Characterization

The X-ray powder diffraction patterns were recorded on a Philips 1830 diffractometer using Cu K $\alpha$  radiation. The diffractograms were recorded in the 2 $\theta$  range of 1-10 with a 2 $\theta$  step size of 0.01° and a step time of 1 s.

Adsorption-desorption isotherms of the synthesized samples were measured at 77 K on micromeritics model ASAP 2010 sorptometer to determine an average pore diameter. Pore-size distributions were calculated by the Barrett-Joyner-Halenda (BJH) method [22], while surface area of the sample was measured by Brunauer-Emmet-Teller (BET) method. SEM images were obtained with JEOL 6300F SEM.

## Batch Adsorption Equilibrium Experiments

Batch adsorption experiments were conducted in order to evaluate the effects of the pH of the solution, adsorbent dose and MG initial concentration. In each batch, the mixture of 25 ml dye solution of known pH and concentration, and a known amount of mesoporous carbon was taken in 50 ml stoppered conical flask and mechanically agitated in a water bath shaker at a constant temperature. After reaching equilibrium, the mixture was filtered. The dye filtrate was then analyzed using a UV spectrophotometer (UV mini 1240 shimadzu) by measuring the absorbance at a wavelength corresponding to maximum absorbance, namely  $\lambda_{\max} = 614$  nm (experimentally obtained by us). The effect of the pH of the solution on MG removal was investigated over a pH range of 3-10. The pH was adjusted using 0.10 M HCl or 0.10 M NaOH aqueous solutions.

The experiments were also carried out by varying the amount of adsorbents (0.001-0.01 g/25 ml) and the concentration of dye solution (10-100 mg l<sup>-1</sup>). For adsorption isotherm, dye solutions of different concentrations (10-100 mg l<sup>-1</sup>) were shaken with a known amount of adsorbent (0.005 g) till the equilibrium was achieved, and then the residual MG concentration of the solution was determined. The amount of adsorbed MG per gram OMC at equilibrium,  $q_e$  (mg g<sup>-1</sup>), was obtained by

$$q_e = \frac{(C_0 - C_e)V}{W} \quad (1)$$

where  $C_0$  and  $C_e$  (mg l<sup>-1</sup>) are the initial and equilibrium

concentrations of MG dye, respectively.  $V$  is the volume of the solution in L and  $W$  is the weight of the adsorbent used in g.

## Adsorption Kinetics of MG

For the measurement of time resolved uptake of MG onto the mesoporous carbon, 5 mg of carbon was introduced into a flask containing 25 ml of MG solution with an initial concentration of 50 mg l<sup>-1</sup> and stirred continuously at 298 K. The concentration of residual MG in the solution was monitored by the same spectrophotometer and the adsorption capacity  $q_t$  was calculated by applying the following equation:

$$q_t = \frac{(C_0 - C_t)V}{W} \quad (2)$$

where  $q_t$  is the adsorption capacity at time  $t$  (mg g<sup>-1</sup>) and  $C_t$  is the concentration of the MG solution at time  $t$  (mg l<sup>-1</sup>).

## Reproducibility and Accuracy of the Results

All batch isotherm experiments were replicated three times and the blanks were run in parallel to establish accuracy, reliability and reproducibility. Blanks were run and corrections applied, if necessary.

## RESULTS AND DISCUSSION

### Physical and Chemical Properties of the Adsorbents

The quality of the MCM-48 and mesoporous carbon prepared in this study was examined by nitrogen adsorption-desorption analysis, X-ray diffraction (XRD) techniques and SEM image. The Nitrogen physisorption is the method of choice to gain knowledge about mesoporous materials. This method gives information on the specific surface area and the pore diameter. Calculating pore diameters of mesoporous materials using the BJH method is common.

Figure 2 shows nitrogen adsorption and desorption isotherms measured at 77 K using a Micromeritics ASAP 2010 automatic analyzer. BET surface areas and the pore size of the synthesized mesoporous sorbents (MCM-48 and OMC) were determined employing BJH (Barrett, Joyner, and Halenda) method via the adsorption branches of the isotherms. The two mesoporous materials yielded a type IV isotherm. The type IV isotherm (IUPAC classification) is typical for mesoporous systems. Table 1 summarizes the important

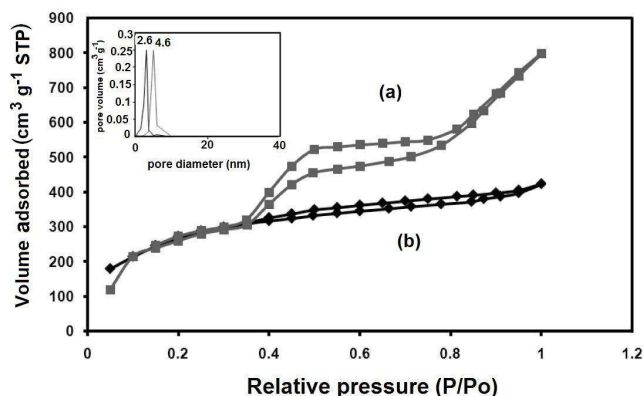


**Fig. 2.** Adsorption-desorption isotherms of nitrogen at 77 K on (a) MCM-48 and (b) OMC.

physical properties of mesoporous sorbents. The surface areas of MCM-48 and OMC samples were 573.1, and 1010.5  $\text{m}^2 \text{g}^{-1}$ , and their average pore size were 46 and 26 Å, respectively. This result mainly depends on the pore size and shape for the silica and carbon materials.

In order to check the structural degradation, XRD data of MCM-48 and OMC were obtained on Philips 1830 diffractometer using Cu K $\alpha$  radiation of wavelength 0.154 nm. Figure 3 shows the XRD peaks of the samples. The XRD patterns of MCM-48 showed two characteristic (211) and (220) reflections in the  $2\theta$  range from  $1^\circ$  to  $10^\circ$ , indicating a well-ordered cubic pore [15]. Like MCM-48, the XRD patterns of OMC showed three diffraction peaks that can be indexed to (110), (210) and (220) in the  $2\theta$  range from  $1^\circ$  to  $10^\circ$ , representing well-ordered cubic pores. The observed data from the original samples of MCM-48 and OMC are in good agreement with that previously reported [21].

Scanning electron microscopy images of mesoporous silica (MCM-48) sample are shown in Fig. 4a. The micrographs clearly revealed that the resulting particles were almost perfectly spherical in shape. The Scanning electron microscopy showed that the porous carbon particles retained the crystal morphologies for the silica template as shown in Fig. 4b. However, the template synthesis did not follow a simple replication process for the structure of the mesoporous silica.

**Table 1.** Textural Parameters of the MCM-48 and OMC Employed in this Study

Adsorbent	d spacing (nm)	$A_{\text{BET}}$ ( $\text{m}^2 \text{g}^{-1}$ )	$V_p$ ( $\text{cm}^3 \text{g}^{-1}$ )
MCM-48	4.6	573.1	0.74
OMC	2.6	1010.5	0.69

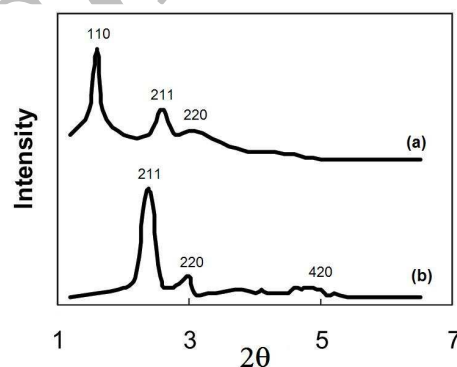


**Fig. 3.** XRD pattern of (a) OMC and (b) MCM-48.

### Adsorption Studies

**Effect of contact time and concentration.** The adsorbate concentration and contact time between adsorbent and adsorbate species play a significant role in the removal of pollutants from water and wastewater by adsorption at a particular temperature and pH. A rapid uptake of pollutant (dye) and establishment of equilibrium in a short period signifies the efficiency of the adsorbent for its use in wastewater treatment.

In order to establish equilibration time for maximum uptake and to know the kinetics of adsorption process, the adsorption of malachite green on carbonaceous adsorbent and MCM-48 was studied as a function of contact time and results are shown in Fig. 5. It is clear from Fig. 5 that the extent of adsorption is rapid in the initial stages and becomes slow in later stages till saturation is attained. This is obvious from the fact that a large number of surface sites are available for adsorption at the initial stages and after a lapse of time, the

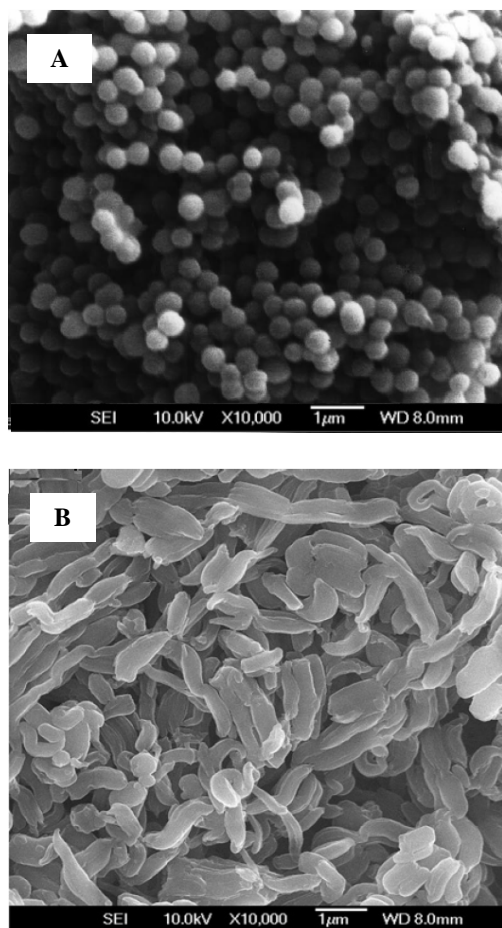


Fig. 4. SEM photographs of (a) MCM-48 and (b) OMC.

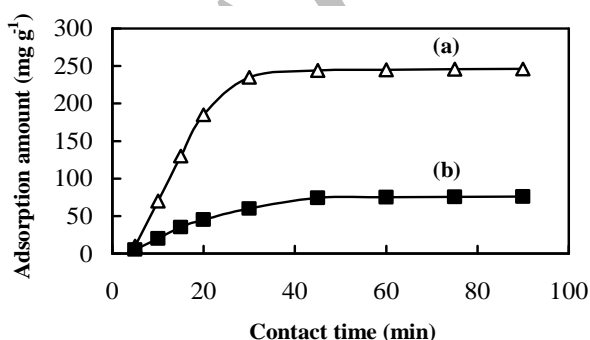


Fig. 5. Effect of contact time on removal of malachite green by adsorbents (a) OMC, (b) MCM-48 ( $C_0 = 50 \text{ mg l}^{-1}$ , adsorbent dosage =  $0.2 \text{ g l}^{-1}$ ,  $T = 298 \text{ K}$ ).

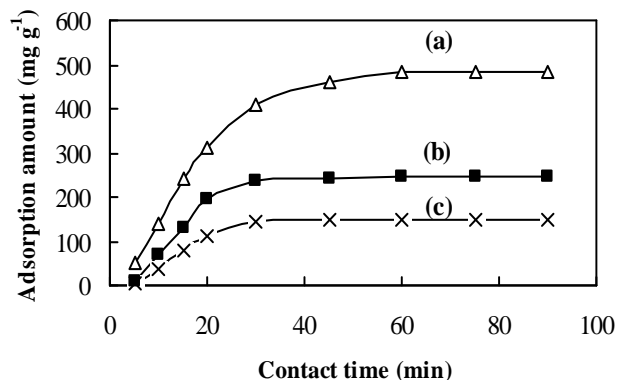


Fig. 6. Effect of initial MG concentration on its uptake on  $0.2 \text{ g l}^{-1}$  mesoporous carbon adsorbent at  $298 \text{ K}$  and different initial concentrations: (a)  $100 \text{ ppm}$ , (b)  $50 \text{ ppm}$ , (c)  $30 \text{ ppm}$ .

remaining surface sites are difficult to be occupied because of repulsion between the solute molecules of the solid and bulk phases. Figure 5 also indicates that the time required for equilibrium adsorption was 30 min. Thus, for all equilibrium adsorption studies, the equilibration period was kept 1 h.

The effect of  $C_0$  on the removal of MG by mesoporous carbon adsorbent is shown in Fig. 6. From the figure, it is evident that the amount of MG adsorbed per unit mass of adsorbent increased with the increase in  $C_0$ . It was found that the time of equilibrium as well as time required to achieve a definite fraction of equilibrium adsorption is independent of initial concentration.

**Effect of pH on dye adsorption.** The experiments were conducted at  $50 \text{ mg l}^{-1}$  initial dye concentration with  $0.005 \text{ g}$  adsorbent mass at  $298 \text{ K}$  for 60 min equilibrium time. Figure 7 shows the effect of pH on the adsorption of MG by mesoporous carbon. It can be seen that dye adsorption was unfavorable at  $\text{pH} < 4$ . The decrease in the adsorption with decrease in pH may be attributed to two reasons. As pH of the system decreased, the number of negatively charged adsorbent sites decreased and the number of positively charged surface sites increased, which did not favor the adsorption of positively charged dye cations due to electrostatic repulsion. While, the lower adsorption of MG at acidic pH is due to the presence of the excess  $\text{H}^+$  ions competing with dye cations for

the adsorption sites of mesoporous carbon. It is known that pH can affect the structural stability of MG and consequently its color intensity [23]. It may be due to the structural changes of MG molecules at high pH. Hence, the dye removal increased sharply over a pH range of 8-10.

**Effect of adsorbent dosage.** The effect of adsorbent dosage on the adsorptive removal of MG by mesoporous carbon is shown in Fig. 8. As it can be seen, adsorption of MG increased with increasing the amount of mesoporous carbon and remained almost constant after increasing up to a certain limit. This can be attributed to increased adsorbent surface area and availability of more adsorption sites [24,25]. The optimum dosage was found to be 0.005 g/25 ml, as the dye removal was 98.2%.

**Kinetic modeling.** In present study, the sorption data were analyzed using two simplest kinetic models; first and second-order models that are explained as follows.

The pseudo first-order equation is expressed as [26,27]:

$$\ln(q_e - q_t) = \ln q_e - k_1 t \quad (3)$$

where  $q_e$  and  $q_t$  are amounts of dye adsorbed ( $\text{mg g}^{-1}$ ) at equilibrium and time  $t$  (min), respectively, and  $k_1$  is the rate constant of pseudo first-order adsorption ( $\text{min}^{-1}$ ). The values of  $\log(q_e - q_t)$  were calculated from the kinetic data of Fig. 9. The values of  $k_1$  and  $q_e$  were calculated from the slope and intercept of the plots of  $\log(q_e - q_t)$  vs.  $t$  for different concentrations. The resulting values together with correlation coefficients are given in Table 2. Also, the calculated  $q_e$  values agree with the experimental data ( $q_{e,\text{exp}}$ ). The results indicate that the adsorption perfectly complies with Pseudo first-order reaction.

The pseudo second-order kinetic model [28,29] is:

$$\frac{t}{q_t} = \frac{1}{k_2 q_e^2} + \left(\frac{1}{q_e}\right)t \quad (4)$$

where  $k_2$  is the rate constant of pseudo second-order adsorption ( $\text{g (mg min)}^{-1}$ ). The  $q_e$  and  $k_2$  values were calculated from slope and intercept of the  $t/q$  vs.  $t$  plots (Fig. 10), respectively. The  $q_{e,\text{exp}}$  values did not agree with calculated ones obtained from the plots. These results showed that the adsorption of MG onto mesoporous carbon is not a

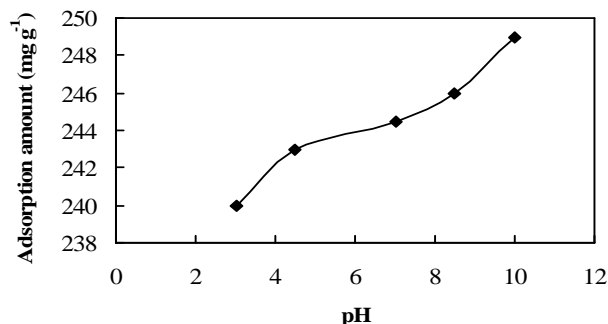


Fig. 7. Effect of pH on equilibrium uptake of malachite green on mesoporous carbon adsorbent. Conditions:  $C_0 = 50 \text{ mg l}^{-1}$ , adsorbent dosage =  $0.2 \text{ g l}^{-1}$ ,  $T = 298 \text{ K}$ .

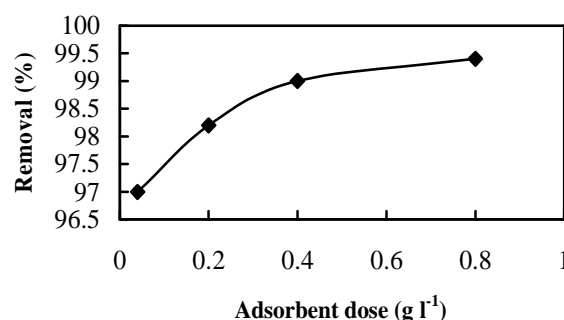


Fig. 8. Effect of adsorbent dosage on the adsorption of MG by mesoporous carbon. Conditions:  $C_0 = 50 \text{ mg l}^{-1}$ ,  $\text{pH} = 8.5$ ,  $T = 298 \text{ K}$ .

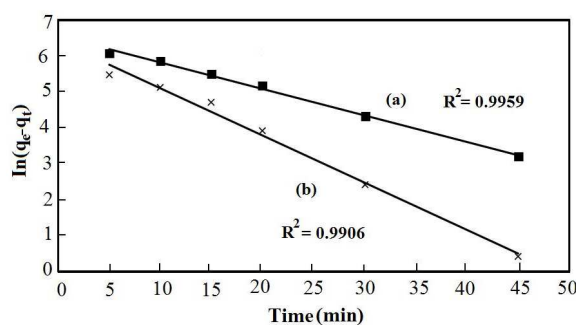
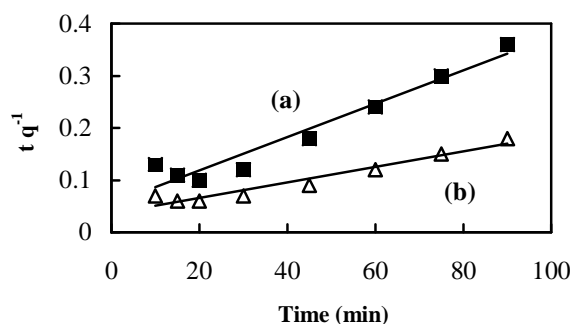
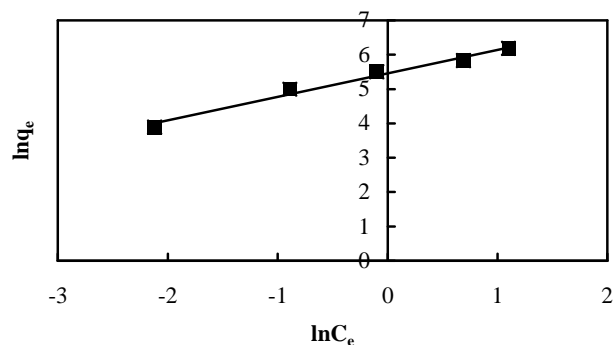


Fig. 9. Pseudo-first order kinetics plots for the removal of malachite green (a) 100 ppm, (b) 50 ppm by mesoporous carbon. Conditions: adsorbent dosage =  $0.2 \text{ g l}^{-1}$ ,  $T = 298 \text{ K}$ ,  $\text{pH} = 8.5$ .

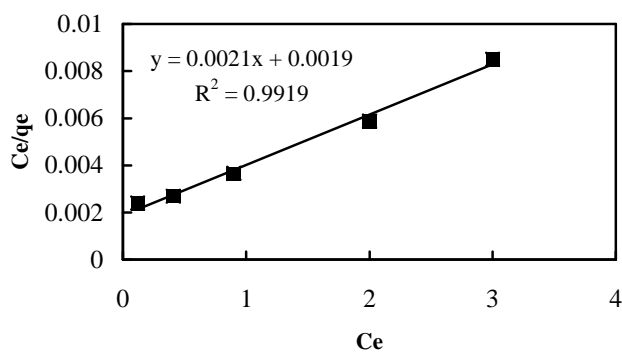
**Table 2.** Pseudo-First Order and Pseudo-Second Order Constants for the Removal of MG by Mesoporous Carbon Adsorbent

$C_0$ ( $\text{mg l}^{-1}$ )	$q_{e, \text{exp}}$ ( $\text{mg g}^{-1}$ )	Pseudo-first order constants			Pseudo-second order constants		
		$q_{e, \text{cal}}$ ( $\text{mg g}^{-1}$ )	$k_1$ ( $\text{g mg}^{-1} \text{min}^{-1}$ )	$R^2$	$q_{e, \text{cal}}$ ( $\text{mg g}^{-1}$ )	$k_2$ ( $\text{g mg}^{-1} \text{min}^{-1}$ )	$R^2$
50	245	312.5	$1.88 \times 10^{-4}$	0.9959	603.11	0.1315	0.9408
100	485	566	$6.33 \times 10^{-5}$	0.9906	694.22	0.0734	0.9432

**Fig. 10.** Pseudo-second order kinetics plots for the removal of malachite green (a) 100 ppm, (b) 50 ppm by mesoporous carbon. Conditions: adsorbent dosage =  $0.2 \text{ g l}^{-1}$ ,  $T = 298 \text{ K}$ ,  $\text{pH} = 8.5$ .**Fig. 11.** Freundlich Isotherm for adsorption of MG on mesoporous carbon adsorbent  $Y = 0.6857x + 5.4613$ ,  $R^2 = 0.9815$ .

pseudo second-order reaction. Table 2 shows that the  $1/n$  is a measure of the adsorption intensity [28]. Figures 11 and 12 show the fitted equilibrium data in Freundlich and Langmuir isotherms.

The fitting results, *i.e.* isotherm parameters and the coefficients of determination,  $R^2$ , are summarized in Table 3. It can be seen that Langmuir isotherm fits the data better than Freundlich isotherm. This is also confirmed by the high value of  $R^2$  in case of Langmuir (0.9919) compared to Freundlich (0.9815) and this indicates that the adsorption of MG on mesoporous carbon takes place as mono-layer adsorption on a surface that is homogeneous in adsorption affinity. The mesoporous carbon adsorbent used in this work had a relatively large adsorption capacity ( $476.1 \text{ mg g}^{-1}$ ). This

**Fig. 12.** Langmuir Isotherm for adsorption of MG on mesoporous carbon adsorbent.

**Table 3.** Isotherm Constants for Adsorption of MG on Adsorbents

	Langmuir constants			Freundlich constants		
	$q_m$ (mg g <sup>-1</sup> )	$b$ (l mg <sup>-1</sup> )	$R^2$	$K_F$ (mg g <sup>-1</sup> )	$n$ (l mg <sup>-1</sup> )	$R^2$
OMC	476.1	1.105	0.9919	235.4	1.4583	0.9815
MCM-48	158.7	0.030	0.9980	9.78	1.7300	0.9910

**Table 4.** Comparison of Adsorption Capacities of Various Adsorbents for Malachite Green

Adsorbent	$q_m$ (mg g <sup>-1</sup> )	(°C)	Ref.
Mesoporous carbon	476.1	25	This work
MCM-48	158.7	25	This work
Activated charcoal	0.179	30	[32]
neem sawdust	4.35	25	[33]
Bentonite clay	7.72	30	[34]
Arundo donax root carbon(ADRC)	8.70	30	[35]
rattan sawdust	62.71	30	[36]
chitosan bead	93.55	30	[37]
Waste apricot	116.27	30	[38]
Rice straw char (RSC)	148.74	30	[39]
Activated carbon	149	25	[40]
Bagasse fly ash (BFA)	170.33	30 ± 1	[25]
Commercially available powdered activated carbon	222.20	30 ± 1	[41]

indicates that mesoporous carbon is effective to remove MG correlation coefficients of first-order kinetic model are greater than second order kinetic.

**Equilibrium isotherms.** Two commonly used isotherms, Langmuir [30] and Freundlich [31], were employed in the present study. The nonlinear Langmuir and Freundlich isotherms are represented by Eqs. (5) and (6):

$$\frac{C_e}{q_e} = \left(\frac{1}{q_m b}\right) + \left(\frac{1}{q_m}\right)C_e \quad (5)$$

$$\ln q_e = \ln k_f + \left(\frac{1}{n}\right)\ln C_e \quad (6)$$

where  $C_e$  (mg l<sup>-1</sup>) is the equilibrium concentration,  $q_e$  (mg g<sup>-1</sup>) is the amount of dye adsorbed at equilibrium, and  $q_m$  (mg g<sup>-1</sup>) and  $K_a$  (l mg<sup>-1</sup>) are Langmuir constants related to adsorption capacity and energy of adsorption, respectively.  $K_F$  (mg g<sup>-1</sup>)(l mg<sup>-1</sup>)<sup>1/n</sup> is the Freundlich adsorption constant and from aqueous solutions.

It is seen from Table 3 that, the order of adsorption in terms of amount adsorbed (mg g<sup>-1</sup>) on different adsorbents is: OMC > MCM-48. This appears due to carbonaceous adsorbent which has higher carbon content, more porosity and high surface area as compared to silica based adsorbents.



### Comparison of Various Adsorbents

Table 4 compares the adsorption capacity of different types of adsorbents used for removal of malachite green. The most important parameter to compare is the Langmuir  $q_m$  value, since it is a measure of adsorption capacity of the adsorbent. The value of  $q_m$  in this study is larger than those in most of previous works. This suggests that MG could be easily adsorbed on mesoporous carbon. The results indicated that the mesoporous carbon can be considered a promising adsorbent for the removal of MG from aqueous solutions.

### CONCLUSIONS

In this work, mesoporous carbon was utilized for the removal of a cationic dye malachite green (MG) from aqueous solution that was prepared by cubic mesoporous silica MCM-48. The structural order and textural properties of synthesized materials were also studied by XRD, SEM and nitrogen adsorption-desorption analysis. Mesoporous carbon showed significant adsorption capacity for malachite green dye under suitable experimental conditions and hence can be recommended as a useful adsorbent. The adsorption was independent of operating variables including solution pH, carbon dose and initial MG concentration. The effective pH and the optimum adsorbent dose were found to be 7-9 and 0.005 g/25 ml, respectively. The Langmuir adsorption isotherm was found to have the best fit to the experimental data, suggesting monolayer adsorption on a homogenous surface. The maximum adsorption capacity of 476.1 mg g<sup>-1</sup> was calculated from Langmuir isotherm. The adsorption kinetics can be predicted by the pseudo-first-order model. It was found that for a short time period the rate of adsorption is controlled by film diffusion.

### REFERENCES

- [1] D.J. Alderman, *J. Fish Dis.* 8 (1985) 289.
- [2] R.F.P. Nogueira, M.R.A. Silva, A.G. Trovó, *Solar Energy* 79 (2005) 384.
- [3] K. Wu, Y. Xie, J. Zhao, H. Hidaka, *J. Mol. Catal. A: Chem.* 144 (1999) 77.
- [4] C. Hachem, F. Bocquillon, O. Zahraa, M. Bouchy, *Dyes Pigm.* 49 (2001) 117.
- [5] H. Kominami, H. Kumamoto, Y. Kera, B. Ohtani, *J. Photochem. Photobiol., A* 160 (2003) 99.
- [6] F. Sayilkan, M. Asiltürk, P. Tatar, N. Kiraz, E. Arpac, H. Sayilkan, *J. Hazard. Mater.* 144 (2007) 140.
- [7] V. Fierro, V. Torne-Fernandez, A. Celzard, *Micropor. Mesopor. Mater.* 92 (2006) 243.
- [8] R.L. Tseng, S.K. Tseng, *J. Colloid Interf. Sci.* 287 (2005) 428.
- [9] M. Hirata, N. Kawasaki, T. Nakamura, K. Naohito, N. Takeo, K. Matsumoto, M. Kabayama, T. Tamura, S. Tanada, *J. Colloid Interf. Sci.* 254 (2002) 17.
- [10] S. Wang, Z.H. Zhu, A. Coomes, F. Haghseresht, G.Q. Lu, *J. Colloid Interf. Sci.* 284 (2005) 440.
- [11] M. Anbia, M. Lashkari, *Chem. Eng. J.* 150 (2009) 555.
- [12] M. Anbia, K. Mohammadi, *Chin. J. Chem.* 26 (2008) 2051.
- [13] M. Anbia, M.K. Rofouei, S.W. Husain, *Asian J. Chem.* 19 (2007) 3862.
- [14] M. Anbia, M.K. Rofouei, S.W. Husain, *Chin. J. Chem.* 24 (2006) 1026.
- [15] S. Jun, S.H. Joo, R. Ryoo, M. Kruk, M. Jaroniec, Z. Liu, T. Ohsuna, O. Terasaki, *J. Am. Chem. Soc.* 122 (2000) 10712.
- [16] B. Sakintuna, Y. Yurum, *Ind. Eng. Chem. Res.* 44 (2005) 2893.
- [17] M. Anbia, S.E. Moradi, *Chem. Eng. J.* 148 (2009) 452.
- [18] M. Anbia, S.E. Moradi, *Appl. Surf. Sci.* 255 (2009) 5041.
- [19] M. Anbia, K. Mohammadi, *Asian J. Chem.* 21 (2009) 3347.
- [20] Y. Shao, L. Wang, J. Zhang, M. Anpo, *J. Phys. Chem.* 109 (2005) 20835.
- [21] R. Ryoo, S.H. Joo, S. Jun, *J. Phys. Chem. B* 103 (1999) 7743.
- [22] U. Ciesla, F. Schouth, *Micropor. Mesopor. Mater.* 27 (1999) 131.
- [23] R. Sun, J. Tomkinson, *Sep. Purif. Technol.* 24 (2001) 529.
- [24] V.K. Garg, R. Kumar, R. Gupta, *Dyes Pigm.* 62 (2004) 1.
- [25] I.D. Mall, V.C. Srivastava, N.K. Agarwal, I.M. Mishra, *Colloid Surf., A* 264 (2005) 17.
- [26] T. Robinson, B. Chandran, P. Nigam, *Bioresour.*

- Technol. 85 (2002) 119.
- [27 ] P.K. Malik, Dyes Pigm. 56 (2003) 239.
- [28 ] Y.S. Ho, G. McKay, Chem. Eng. J. 70 (1998) 115.
- [29 ] Y.S. Ho, G. McKay, Process Biochem. 34 (1999) 461.
- [30 ] I. Langmuir, J. Am. Chem. Soc. 38 (1916) 2221.
- [31 ] H.M.F. Freundlich, J. Phys. Chem. 57 (1906) 385.
- [32 ] M.J. Iqbal, M.N. Ashiq, J. Hazard. Mater. B139 (2007) 57.
- [33 ] S.D. Khattri, M.K. Singh, J. Hazard. Mater. 167 (2009) 1089.
- [34 ] S.S. Tahir, N. Rauf, Chemosphere 63 (2006) 1842.
- [35 ] J. Zhang, Y. Li, Ch. Zhang, Y. Jing, J. Hazard. Mater. 150 (2008) 774.
- [36 ] B.H. Hameed, M.I. El-Khaiary, J. Hazard. Mater. 159 (2008) 574.
- [37 ] Z. Bekçi, C. Özveri, Y. Seki, K. Yurdakoç, J. Hazard. Mater. 154 (2008) 254.
- [38 ] C.A. Basar, J. Hazard. Mater. B135 (2006) 232.
- [39 ] B.H. Hameed, M.I. El-Khaiary, J. Hazard. Mater. 153 (2008) 701.
- [40 ] Y. Önal, C. Akmil-Başar, Ç. Sarıcı-Özdemir, J. Hazard. Mater. 146 (2007) 194.
- [41 ] R. Malik, D.S. Ramteke, S.R. Wate, Waste Manage. 27 (2007) 1129.